

# INVESTIGATIONS OF LONG-RANGE WAKEFIELD EFFECTS IN A TESLA-TYPE CRYOMODULE AT FAST\*

A. H. Lumpkin<sup>#</sup>, R. Thurman-Keup, D. Edstrom Jr., P. Prieto, J. Ruan  
Fermi National Accelerator Laboratory, Batavia, IL 60510 USA  
B. Jacobson, J. Sikora, J. Diaz-Cruz<sup>1</sup>, A. Edelen, F. Zhou  
SLAC National Accelerator Laboratory, Menlo Park, CA 94025 US  
<sup>1</sup>also at University of New Mexico, Albuquerque, NM 87131 USA

## Abstract

Experiments were performed at The Fermilab Accelerator Science and Technology (FAST) facility to elucidate the effects of long-range wakefields (LRWs) in TESLA-type rf cavities. In particular, we investigated the higher-order modes (HOMs) generated in the eight cavities of a cryomodule (CM) due to off-axis steering with correctors H/V 125 located ~4 m upstream of the CM. We have observed correlated submacropulse centroid slews of a few-hundred microns and centroid oscillations at ~240 kHz in the rf BPM data after the CM. The entrance energy was 25 MeV, and the exit energy was 100 MeV with 125 pC/b in a 50-bunch train. These experiments will be used to inform the commissioning plan for the LCLS-II injector CM.

## INTRODUCTION

An ongoing challenge at large facilities is the preservation of the low emittance of electron beams during transport in the accelerating structures. In the cases of the TESLA-type superconducting rf cavities currently used in the European X-ray Free-electron Laser (FEL) [1] and the under construction Linac Coherent Light Source upgrade (LCLS-II) [2], off-axis beam transport may result in emittance dilution due to transverse long-range wakefields (LRWs) and short-range wakefields (SRW) [3-5]. To investigate such effects, experiments were performed at the Fermilab Accelerator Science and Technology (FAST) facility with its unique configuration of two TESLA-type cavities after the photocathode rf gun followed by an 8-cavity cryomodule [6].

We generated beam trajectory changes with the H/V125 corrector magnet set located 4 m upstream of the cryomodule. We observed correlations of the cavity higher-order modes (HOMs) signal levels and submacropulse centroid slews and/or centroid oscillations in the 11 BPM locations downstream of the cryomodule. At 125 pC/bunches, 50 bunches per macropulse, 25-MeV entrance energy, and 100-MeV exit energy, we observed for the first time submacropulse position slews of up to 500 microns at locations within 3 m after the CM and a centroid oscillation at a difference frequency of 240 kHz further downstream. Both are emittance-dilution effects which we mitigated with selective upstream beam steering

\*This manuscript has been authored by Fermi Research Alliance, LLC under Contract No. DE-AC02-07CH11359 with the U.S. Department of Energy, Office of Science, Office of High Energy Physics.  
#lumpkin@fnal.gov

The experiments were facilitated by the implementation of two prototype HOM detector chassis designed for the LCLS-II injector cryomodule. These chassis were based on the basic FNAL design with a dipolar mode passband and zero-bias Schottky detectors, but they had additional selectable features for up to two wideband amplifiers in series and attenuators in each channel [7]. The combined 8 channels then enabled one coupler from all eight cavities to be measured at the same time to assess the beam trajectory relative to the cavity-mode centers.

## EXPERIMENTAL ASPECTS

### *The Electron Linac*

The Integrable Optics Test Accelerator (IOTA) electron injector at the FAST facility (Fig. 1) begins with an L-band rf photoinjector gun built around a Cs<sub>2</sub>Te photocathode (PC). When the UV component of the drive laser, described elsewhere [8] is incident on the PC, the resulting electron bunch train with 3-MHz micropulse repetition rate exits the gun at <5 MeV. Following a short transport section with a pair of trim dipole magnet sets, the beam passes through two superconducting rf (SCRF) capture cavities denoted CC1 and CC2, and then a transport section to the low-energy electron spectrometer. In this case this dipole is off so 25-MeV beam is transported to and through the CM with an exit energy of 100 MeV. Diagnostics used in these studies include the rf BPMs and HOM couplers at the upstream (US) and downstream (DS) ends of each SCRF cavity. There are thus 16 couplers within the CM. The HOM signals were processed by the HOM detector circuits with the Schottky diode output provided online through ACNET, the Fermilab accelerator controls network [4]. The HOM detectors' bandpass filters were optimized for two dipole passbands from 1.6 to 1.9 GHz, and the 1.3-GHz fundamental was reduced with a notch filter. With the implementation of the SLAC prototype HOM chassis with 8 channels in total [7], we could cover all 8 US or 8 DS couplers at one time as schematically shown in Fig. 5 of reference [7] in this conference. In addition, a hybrid FNAL HOM chassis provided three filtered outputs centered at 1.75, 2.58, and 3.25 GHz of two channels on the unused C1 and C8 outputs. Two 12-channel, 10-bit digitizers provided by FNAL established the link to the ACNET system. The rf BPMs' electronics were configured for bunch-by-bunch capability with optimized system attenuation for each charge.

Content from this work may be used under the terms of the CC BY 3.0 licence (© 2021). Any distribution of this work must maintain attribution to the author(s), title of the work, publisher, and DOI

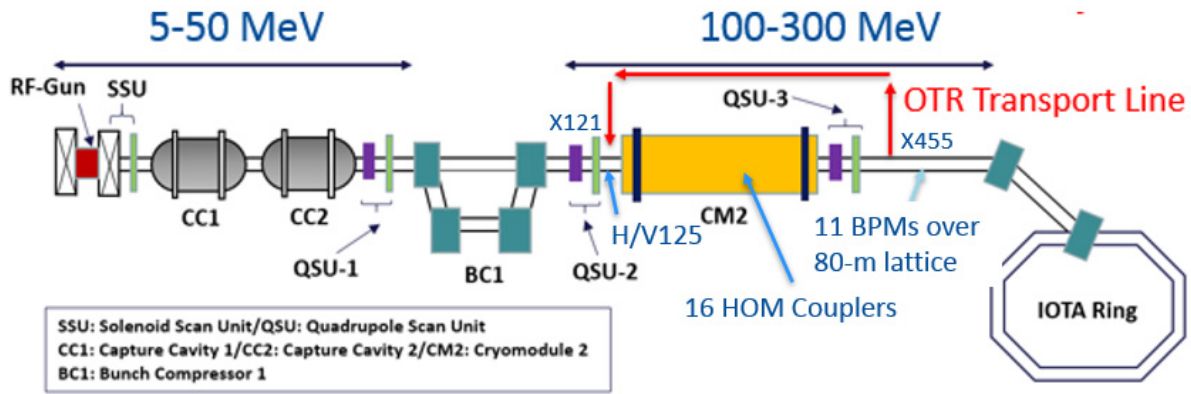


Figure 1: Schematic of the FAST/IOTA beamline layout showing the PC rf gun, capture cavities (CCn), BC1 chicane, X121 OTR and YAG:Ce screens, the cryomodule (CM), high-energy transport line, and the IOTA ring. The Low Energy and High Energy absorbers are not shown.

## EXPERIMENTAL RESULTS

### Initial CM2 HOM Waveform Data: 125 pC/b

An assessment of beam offset in the CM2 cavities was provided by the HOM data, both upstream (US) and downstream (DS) signals. Examples of initial digitized waveforms are shown in Fig. 2. The CM2 HOM signals were surprisingly weaker than those of the single cavities, CC1 and CC2 at this charge. When no amplifiers were used, we see only the C3 and C4 US HOM waveforms, green and yellow, respectively visibly above the baseline in Fig. 2a. The use of a single wideband amplifier on each channel then made all 8 signals measurable in Fig. 2b. Steering with the corrector V125 located just 4 m before CM2 (see Fig.1) results in the correlated trajectory and HOM signal changes. The steering is  $\sim 2\text{mrad/A}$  into CM2. Our reference currents were  $H125=1.5\text{ A}$  and  $V125=4.3\text{ A}$ . Peak-value data with corrector current scans are shown in a companion paper [7].

### HOM CM2 Spectral Data

In a new initiative, we operated with a single bunch to explore the detailed spectral information obtainable with a Rohde & Schwartz 20 GS/s oscilloscope [9]. The filtered HOM signals were directly recorded for 15-20  $\mu\text{s}$  after the beam trigger for the 18 dipolar modes in the passband. Figure 3 shows an example of the FFT of the temporal digital data near 1.726 GHz. In this case of the CM:C1 US dipole mode 7, we resolve the horizontal and vertical polarization components with the horizontal component clearly changing during the H125 scan from -1 to +1 A. The frequency splitting is more than 2 MHz for this Advanced Engineering Systems (AES)-built cavity. The cavity is not axisymmetric evidently.

As another example we show the C8 mode 7 near 1.730 GHz in Fig. 4. In this RI-built cavity, the frequency splitting is only 1 MHz, and only the vertical component changes amplitude with the V125 scan values.

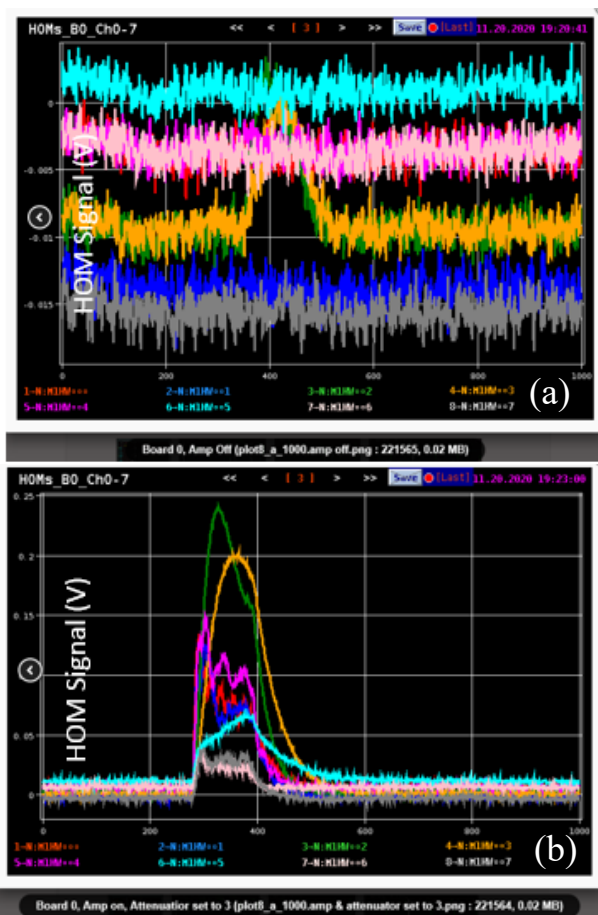


Figure 2: (a) Initial US HOM waveforms for Cavities 1-8 with colors red, blue, green, yellow, purple, light blue, pink, and grey, respectively. Only C3 and C4 seem to have usable signals with no amplifier. (b) The US HOM signals with one wideband amplifier switched on. All 8 Schottky detector signals are now measurable on the same shot. These are the dipolar modes with 50 b and 16.6  $\mu\text{s}$  extent.

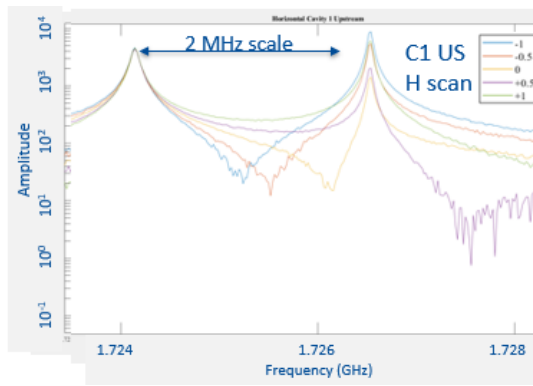


Figure 3: Example frequency spectral content with two polarization components of C1 US mode 7 resolved near 1.726 GHz. Only the horizontal component is responsive to the H125 scan.

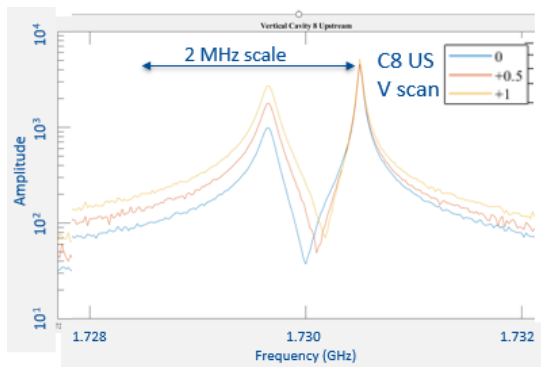


Figure 4: Example frequency spectral content with two polarization components of C8 US mode 7 resolved near 1.730 GHz. Only the vertical polarization component is responsive to the V125 scan.

### Bunch by Bunch rf BPM Data: 125 pC/b

We also evaluated the potential long-range wakefield or HOM effects on the beam centroid by using the rf BPM data. These data were obtained in an off-normal condition with CC2 tuned 15 kHz off-resonance and powered off. This is discussed elsewhere in these proceedings [10].

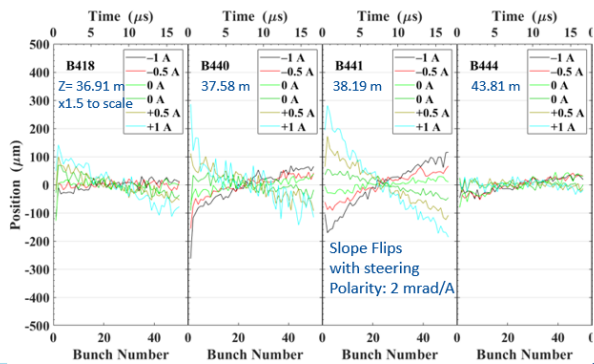


Figure 5: Submacropulse vertical centroid effects in the first four BPM locations after CM2:C8 correlated V125 settings. This includes the cold BPM denoted B418. The z-locations are shown in each panel with the maximum centroid slewing seen in B441.

The beam energy is 25 MeV entering and 100 MeV exiting CM2. An example of the centroid motion within the 50-micropulse train in a macropulse is shown in Fig. 5 with both noise-reduction and bunch-by-bunch capabilities implemented. The first three vertical BPMs after CM2:C8 show an increasing (and correlated with V125 settings) centroid slew which grows to 500  $\mu\text{m}$  in B441. B418 is the cold BPM located just after C8 and still within the CM. Further downstream we show samples from B480 where a vertical centroid oscillation of  $\sim 240$  kHz is seen in Fig. 6 for the larger -1 A V125 corrector values. In this preliminary set, we did not have an offset minimum established at 0.0 A from the reference although the oscillation amplitude is noticeably larger at -1 A.

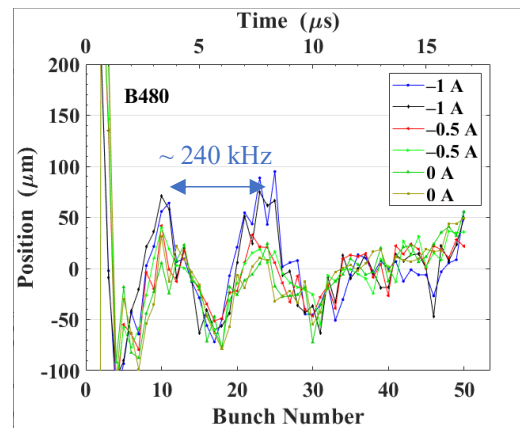


Figure 6: Examples of the variation of the beam vertical centroids bunch by bunch for 50 micropulses at B480. The  $\sim 240$  kHz centroid oscillation is indicated.

## SUMMARY

In summary, the HOM detectors and rf BPMs were used to evaluate off-axis steering effects in a cryomodule for the first time at FAST. Significant submacropulse centroid slewing and in some cases, oscillations were observed downstream of the CM and correlated with steering purposely off axis into the CM. The emittance-dilution effects could be mitigated by minimizing the HOMs and the slewing effects. These effects are being evaluated for machine learning training [11] with a goal to preserve the emittance of bright beams in the LCLS-II injector.

## ACKNOWLEDGMENTS

The Fermilab authors acknowledge the support of C. Drennan, A. Valishev, D. Broemmelsiek, G. Stancari, and M. Lindgren, all in the Accelerator Division at Fermilab. The SLAC/NAL authors acknowledge the support of J. Schmerge (Superconducting Linac Division, SLAC).

## REFERENCES

- [1] H. Weise and W. Decking, “Commissioning and First Lasing of the European XFEL”, in *Proc. 38th Int. Free Electron Laser Conf. (FEL'17)*, Santa Fe, NM, USA, Aug. 2017, pp. 9-13. doi:10.18429/JACoW-FEL2017-MOC03
- [2] P. Emma, “Status of the LCLS-II FEL Project at SLAC”, in *Proc. 38th Int. Free Electron Laser Conf. (FEL'17)*, Santa Fe, NM, USA, Aug. 2017, Talk, JACoW-FEL2017-MOD01
- [3] J. T. Seeman *et al.*, “Transverse Wakefield Control and Feedback in the SLC Linac”, in *Proc. 12th Particle Accelerator Conf. (PAC'87)*, Washington D.C., USA, Mar. 1987, pp. 1349-1353.
- [4] A. H. Lumpkin *et al.*, “Submacropulse electron-beam dynamics correlated with higher-order modes in Tesla-type superconducting rf cavities”, *Phys. Rev. Accel. Beams*, vol. 21, no. 6, p. 064401, Jun. 2018. doi:10.1103/physrevaccelebeams.21.064401
- [5] A. H. Lumpkin, R. M. Thurman-Keup, D. Edstrom, and J. Ruan, “Submicropulse electron-beam dynamics correlated with short-range wakefields in Tesla-type superconducting rf cavities”, *Phys. Rev. Accel. Beams*, vol. 23, no. 5, p. 054401, May 2020. doi:10.1103/physrevaccelebeams.23.054401
- [6] M. Church *et al.*, “The ASTA User Facility Proposal”, Fermi National Accelerator Laboratory, Batavia, IL, Rep. Fermilab-TM-2568, Oct. 2013.
- [7] J. Sikora *et al.*, “Commissioning of the LCLS-II Prototype HOM Detectors on TESLA-type Cavities at FAST”, presented at IPAC'21, Campinas, Brazil, paper MOPAB323, this conference.
- [8] J. Ruan, M. D. Church, D. R. Edstrom, T. R. Johnson, and J. K. Santucci, “Commissioning of the Drive Laser System for Advanced Superconducting Test Accelerator”, in *Proc. 4th Int. Particle Accelerator Conf. (IPAC'13)*, Shanghai, China, May 2013, paper WEPME057, pp. 3061-3063.
- [9] R. Thurman-Keup *et al.*, “Observation of Polarization-Dependent Changes in Higher-Order Mode Responses as Function of Transverse Beam Position in Tesla-Type Cavities at FAST”, presented at IPAC'21, Campinas, Brazil, paper MOPAB232, this conference.
- [10] A. H. Lumpkin *et al.*, “Observations of Long-range Wakefield Effects Generated in an Off-Resonance Tesla-TypeCavity”, presented at IPAC'21, Campinas, Brazil, paper TUPAB272, this conference.
- [11] J. Diaz-Cruz *et al.*, “Machine Learning Training for HOM reduction and Emittance Preservation in a TESLA-type Cryomodule at FAST”, presented at IPAC'21, Campinas, Brazil, paper MOPAB289, this conference.